JCIS Open 6 (2022) 100048

Contents lists available at ScienceDirect

JCIS Open

journal homepage: www.journals.elsevier.com/jcis-open

Influence of molecular weight and concentration of carboxymethyl cellulose on rheological properties of concentrated anode slurries for lithium-ion batteries

Masahiko Ishii *, Hiroshi Nakamura

Toyota Central Res. & Develop. Labs., Inc., Yokomichi 41-1, Nagakute, Aichi, 480-1192, Japan

ARTICLE INFO

Keywords:
Lithium-ion battery
Carboxymethyl cellulose
Graphite
Shear thickening

ABSTRACT

The detailed behavior of carboxymethyl cellulose (CMC) as a dispersant in model anode slurries for lithium-ion batteries was investigated. Slurries with different graphite and CMC concentrations using three types of CMCs having different molecular weights were prepared, and changes in viscosity in the low shear rate range together with shear thickening in the high shear rate range were assessed. At a constant CMC concentration, the viscosities at low shear rates decreased as the graphite concentration was increased. Shear thickening was also more evident at low CMC concentrations and when using CMCs with lower molecular weights as well as at high graphite concentrations. These results suggest that, within the CMC concentration range investigated in the present work, the majority of the CMC was adsorbed on the graphite particles and this adsorbed CMC affected the rheological properties of the slurry. Increases in graphite concentration decreased the amount of adsorbed CMC per graphite particle, which in turn lowered the viscosity in the low shear rate range and enhanced shear thickening in the high shear rate range. The adsorbed CMC affected the slurry viscosity via electrostatic and steric interactions at low shear rates and acted as a buffer to inhibit shear thickening at high shear rates, primarily as a result of steric effects.

1. Introduction

Slurries, defined as dispersions of particles or powders in liquids (dispersion media), are widely used for the fabrication of materials and products such as paints, catalysts, batteries and fuel cells. Because the dispersion states and rheological properties of slurries will affect the quality and performance of such products, these parameters should be fully understood and controlled. Recently, slurries having high solids contents have become of interest as a means of improving productivity, because the high solids contents can reduce the load of evaporating dispersion media. However, increasing the solids content typically also increases the viscosity of a slurry and concentrated slurries often exhibit shear thinning. This is a phenomenon in which the viscosity decreases with increases in the shear rate. In addition, the slurries can also show shear thickening, meaning that viscosity increases at relatively high shear rates. Shear thinning allows processing, and is associated with a very high low-shear limit viscosity that limits settling of the particles in the static condition; this set of related rheological behaviors is useful in the formation and shape retention of wet films [1–3]. However, the rheological properties of the slurry must be tailored for each product or process so as to obtain the appropriate viscosities at low and high shear rates [4–6]. In contrast, shear thickening is unacceptable in many applications, other than shockproof materials [7], because this phenomenon can induce clogging of pipes or filters [8–11].

To overcome the above problems, it is necessary for the particles in a slurry to be fully dispersed and to form a network structure in the static state [12], and additives such as dispersants and thickeners are often utilized to achieve these goals. Specific dispersants can promote the formation of a network structure in addition to an appropriate dispersion state as a result of electrostatic repulsion and/or steric interactions introduced by adsorbed dispersant molecules [13]. Sodium carboxymethyl cellulose (CMC) is a water-soluble cellulose derivative comprising anhydroglucose units, each with three hydroxyl groups, in which hydrogen atoms have been partially substituted by sodium carboxymethyl groups. CMC has been used as a thickener or stabilizer in the food, pharmaceutical and cosmetics industries, and the effects of the CMC molecular weight, degree of substitution (DS) and concentration in aqueous dispersions have been intensively studied [14–24]. The

* Corresponding author.
E-mail address: m-ishii@mosk.tytlabs.co.jp (M. Ishii).

https://doi.org/10.1016/j.jciso.2022.100048
Received 6 December 2021; Received in revised form 25 February 2022; Accepted 11 April 2022

existence of several critical concentrations depending on the degree of interaction between CMC molecules has been reported [19,21,23,24]. The rheology of these dispersions has also been found to be affected by both electrostatic and hydrophobic interactions, which can be controlled by varying the DS and salt concentration [14–17].

In addition to functioning as a thickener, CMC can also behave as a dispersant and is commonly used in anode slurries for lithium-ion batteries. A standard anode slurry consists of graphite particles (acting as the negative electrode active material), CMC (as a dispersant), styrene-butadiene rubber (SBR; as a binder) and water (as a dispersion media). Many studies have focused on the effects of CMC on the rheological properties and performance of electrodes fabricated from such slurries [25–31]. Lee et al. determined that CMC will be adsorbed on graphite as a result of hydrophobic interactions and subsequently generates stable dispersions due to both electrostatic and steric effects [27]. In addition, CMC with a low DS of approximately 0.7 has been shown to perform better as a dispersant than samples with larger DS values of more than 1.0 [26]. It has been reported that, at a graphite concentration of 50 wt%, CMC with a DS of 0.7 will be adsorbed on the graphite to a maximum concentration of 1.3% and will subsequently increase the fluidity of the slurry [29]. Gordon et al. found that the CMC in a slurry in which the CMC proportion in the dry electrode is 2.5–4.0 vol% is partially adsorbed and the free CMC in the solvent affects the viscous behavior of the system [31]. Gordon's work also indicated that higher molecular weight CMC exhibits better adsorption on graphite particles.

Although lithium-ion batteries have already been put to practical use in mobile devices, electric vehicles (EVs) and other products, further higher performance and lower cost are required to permit the use of these batteries in future EVs [32]. One means of reducing the cost is to simplify the drying stage by increasing the concentration of the slurry during the electrode fabrication process. In addition, one approach to improving performance is to improve conductivity and capacity of the electrode by reducing the amount of CMC. Therefore, it is important to understand the relationship between the graphite concentration and the amount of CMC in order to obtain high concentration slurries. It would also be helpful to assess the manner in which the action of the dispersant differs depending on variations in the CMC molecular weight. However, there have not been enough systematic investigations concerning the relationship between the graphite concentration and the amount of CMC in the case that the graphite concentration is relatively high and the CMC concentration is relatively low, in conjunction with CMCs having the same DS but different molecular weights.

In this study, we investigated the rheological behavior of anode slurries, focusing on the effect of adsorbed CMC on the viscosities at low shear rates and shear thickening at high shear rates. Therefore, we prepared slurries with different graphite and CMC concentrations using three types of CMCs having different molecular weights, and measured the shear rate dependence of the viscosity and the strain dependence of the elastic moduli for these slurries. We first investigated the low-shear viscosity behaviors of the slurries and found that the low-shear viscosity decreased as the graphite concentration was increased. Next, the effect of the molecular weight and the addition amount of CMC on the shear thickening was demonstrated using the change in elastic moduli. Finally, these results were discussed based on the effect of CMC adsorbed on graphite. In order to simplify the test system and to permit a better understanding of the effect of each CMC, model anode slurries comprising dispersions only of graphite and CMC in water were employed, without SBR.

2. Experimental

2.1. Materials

Graphite particles (OMAC-R1.2Z/SS, Osaka Gas Chemicals, Japan) with an average diameter of 12.4 μm, a specific surface area of 3.45 m^2/g and a density of 2.2 g/cm^3 (based on data provided by the manufacturer) were used as the active material. Three types of CMC were employed (Sunrose, Nippon Paper Group, Japan), all having approximately the same DS but with different weight average molecular weights (Mw). These are denoted herein as CMC-A, -B and -C. The DS values, viscosities of 1 wt% suspensions and estimated Mw values for these materials are summarized in Table 1. The Mw of each specimen was approximated using an equation obtained from a previous publication [30] (see Supplemetary Data).

2.2. Slurry preparation

Both 1 and 2 wt% CMC dispersions were prepared by adding ion-exchanged water to each of the above three types of CMC and stirring with a magnetic stirrer for 1–3 days. Each model anode slurry was prepared by combining quantities of a CMC dispersion, graphite and water so as to have a graphite concentration of 53–59 wt% (33.9–39.5 vol%) and a CMC concentration of 0.2–0.8 wt% (these concentrations are based on total mass of each slurry), followed by stirring of each mixture with a spatula. Subsequently, a rotation/revolution type mixer (Thinky Mixer ARE-310, Thinky, Japan) was used to stir/defoam the mixture at rotation/revolution rates of 800/2000 rpm for 1 min and then 60/2200 rpm for 1 min.

2.3. Rheological measurements

Rheology measurements were performed 1–2 days after each model slurry was prepared. Each slurry was stirred with a spatula for 1–2 min immediately prior to the measurements, after which the slurry was set on the plate of a rheometer (MCR301, Anton Paar, USA) with a gap between the cone (⌀50 mm, 1°) and the plate of 0.1 mm. The effect of shear rate on the sample viscosity was examined under steady flow conditions at 25 °C, with each trial performed twice in succession while increasing and decreasing the shear rate between 10^{-2} and 10^{3} s^{-1}. In the first measurement, the data obtained in the ascending direction were found to be unstable due to the effect of the shear history imparted when loading the slurry into the jig, while the measurements obtained in the descending direction were essentially constant between the first and second measurements. The results obtained from the second descending shear rate experiments are provided below. Following the measurement of the shear rate dependence of the steady flow viscosity, the strain dependence of elastic moduli was assessed based on dynamic viscoelasticity trials in order to quantitatively discuss the magnitude of shear thickening. Specifically, the storage modulus, G′, and loss modulus, G″, were determined over the strain range of 10^{-2} to 10^{3}% at a frequency of 1 Hz (6.28 rad/s). The ratio of the maximum value to the minimum value of G″ in the high strain region of 10^{1}–10^{3}%, G''_{max}/G''_{min} was used as an index to indicate the magnitude of shear thickening.

3. Results

Fig. 1 shows the shear rate dependence of the viscosities of slurries with CMC concentrations of 0.2, 0.4, 0.6 and 0.8 wt% and graphite concentrations of 53, 55, 57 and 59 wt%, as obtained using CMC-A. At a CMC concentration of 0.2 wt% (Fig. 1a), the slurries with graphite

Table 1
Degree of substitution values, viscosities of 1 wt% suspensions and estimated molecular weights of the CMCs used in this work.

CMC	Degree of Substitution	Viscosity of 1 wt% suspension (mPa s)	Estimated Mw (g/mol)
CMC-A	0.70	1290	1.5×10^5
CMC-B	0.70	4940	2.6×10^5
CMC-C	0.69	8800	3.6×10^5

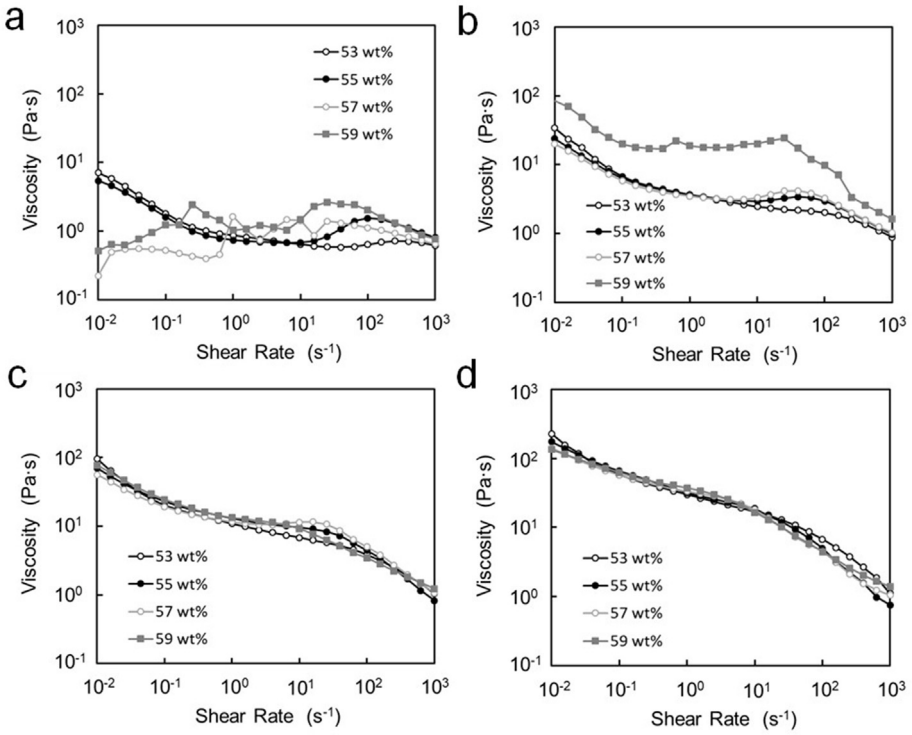

Fig. 1. Viscosities as functions of shear rate for model anode slurries with CMC concentrations of (a) 0.2, (b) 0.4, (c) 0.6 and (d) 0.8 wt% using CMC-A. The wt% values shown in the graphs indicate graphite concentrations.

concentration of 53 and 55 wt% showed weak shear thinning and thickening. The shear thickening on the 55 wt% slurry was stronger than that on the 53 wt% slurry. Viscosities of the 57 and 59 wt% samples were unstable at low shear rates and showed shear thickening at high shear rate. At a CMC concentration of 0.4 wt% (Fig. 1b), there was no significant difference in viscosity at 53, 55 and 57 wt% in the low shear rate range of 10^{-2} to 10^{1} s^{-1}. However, at shear rates above 10^{1} s^{-1}, the viscosity of the 53 wt% slurry decreased monotonically, while the 55 and 57 wt% samples exhibited shear thickening. At 59 wt%, the viscosity was higher and relatively unstable at all shear rates compared with the other

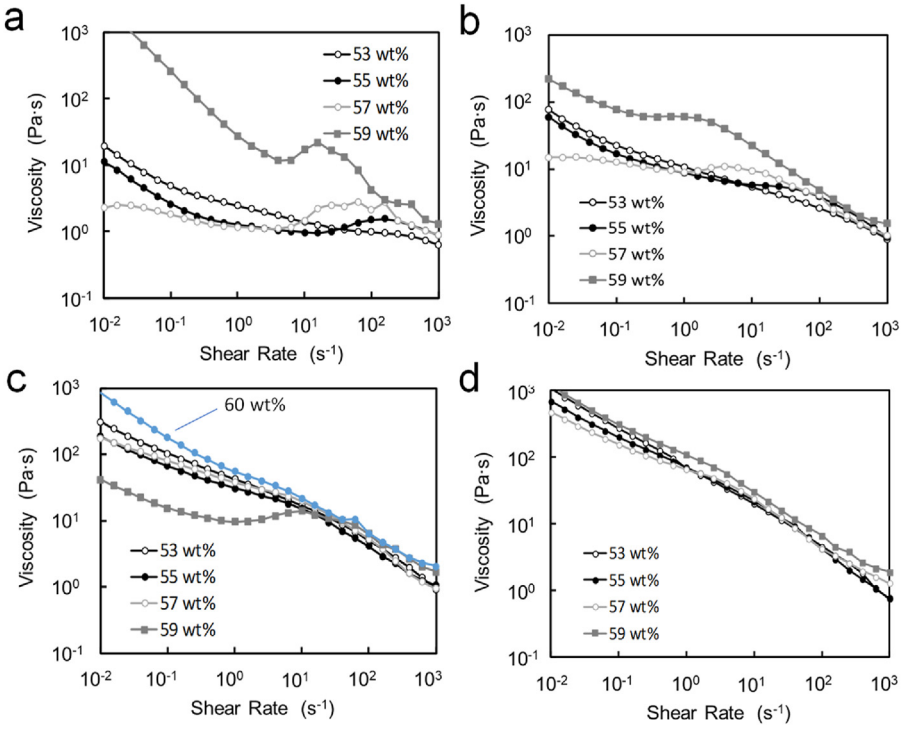

Fig. 2. Viscosities as functions of shear rate for model anode slurries with CMC concentrations of (a) 0.2, (b) 0.4, (c) 0.6 and (d) 0.8 wt% using CMC-B. The wt% values shown in the graphs indicate graphite concentrations.

graphite concentrations. At CMC concentrations of 0.6 and 0.8 wt% (Fig. 1c and d), no significant difference was observed in the shear rate dependence of viscosity at any graphite concentration. Only minimal shear thickening was observed at a CMC concentration of 0.6 wt% and a graphite concentration of 57 wt%.

Fig. 2 summarizes the effects of shear rate on the viscosities of slurries with CMC concentrations of 0.2, 0.4, 0.6 and 0.8 wt% and graphite concentrations of 53, 55, 57 and 59 wt% when using CMC-B. At a CMC concentration of 0.2 wt% (Fig. 2a) and in the low shear rate range of 10^{-2} to 10^{-1} s^{-1}, the viscosity decreased as the graphite concentration was increased from 53 to 55 and then to 57 wt%. In contrast, the viscosity at 59 wt% was higher than the viscosity at 53 wt%. In addition, although the viscosity decreased monotonically with increasing shear rate at a graphite concentration of 53 wt%, at 55 wt% and above, shear thickening was observed at the shear rates from 10^{1} to 10^{2} s^{-1}. This shear thickening occurred at lower shear rates as the graphite concentration was increased. At a CMC concentration of 0.4 wt% (Fig. 2b), the viscosity trends were almost the same as those at 0.2 wt%. However, at 0.6 wt% (Fig. 2c), the viscosity at 59 wt% was lower than that at 53 wt% in the low shear rate range and shear thickening was observed only at 59 wt%. The effects of higher graphite concentrations were assessed by monitoring the viscosity of a 60 wt% slurry, and the results are included in Fig. 2c. At this concentration, the viscosity in the low shear rate range was higher than that at 53 wt% but no significant shear thickening was observed. At a CMC concentration of 0.8 wt% (Fig. 2d), the viscosities at low shear rates in the range of 10^{-2} to 10^{-1} s^{-1} were found to decrease in the order of 53 ≈ 59 > 55 > 57 wt%, similar to the results obtained at other CMC concentrations. In addition, no shear thickening was observed at any graphite concentration.

The effects of shear rate on the viscosities of slurries with CMC concentrations of 0.2–0.8 wt% and graphite concentrations of 53–59 wt% using CMC-C are shown in Fig. 3. Note that the viscosity of the several specimens (CMC-0.6/Graphite-59, 0.8/57, and 0.8/59 wt%) could not be measured because the gap of the measuring jig could not be set to the predetermined value of 0.1 mm due to the extremely high viscosity of the material. At a CMC concentration of 0.2 wt% (Fig. 3a), the slurry with a graphite concentration of 53 wt% showed only shear thinning, and the slurry with a graphite concentration of 55 wt% showed shear thinning and weak thickening. The viscosity of the 57 wt% sample was unstable at low shear rates and showed shear thickening at high shear rate. For the 59% sample, no measurements were taken in anticipation of data instability. At a CMC concentration of 0.4 wt% (Fig. 3b), the viscosities of the 53 and 55 wt% samples showed almost the same effect of shear rate in the shear rate range of 10^{-2} to 10^{1} s^{-1}, although the viscosity of the 57 wt% slurry was lower than both of these samples. In the high shear rate range, only the viscosity of the 53 wt% slurry decreased monotonically, while weak shear thickening was observed at the other graphite concentrations. At CMC concentrations of 0.6 and 0.8 wt% (Fig. 3c and d), the viscosity decreased monotonically and no shear thickening was observed at any of the graphite concentrations. The viscosities of the 55 wt% sample were lower than those of 53 and 57 wt% ones over the entire shear rate range at a CMC concentration of 0.6 wt%.

Generally, a higher solid content will produce a more viscous slurry. However, the above results indicate that increasing the graphite concentration from 53 to 57 wt% lowered the viscosity in the low shear rate range in many cases. To gain some insight into the cause of these phenomena, Fig. 4 shows graphs plotting the relationship between the weight ratio of CMC to graphite and the viscosity at a shear rate of 10^{-2} s^{-1}. In the graphs, in order to clarify the change in the viscosity due to the change in the CMC/graphite ratio, the plot points are connected by a straight line with each CMC concentration as one set for each type of CMC. Fig. 4b is an enlarged view of the part of Fig. 4a where the CMC concentration is 0.2 wt%. The graphs show that at each CMC concentration, the viscosity tends to decrease due to the decrease in the CMC/graphite ratio that is induced by the increase in the graphite concentration. The graphs also show that the viscosity starts to increase as the CMC/graphite ratio becomes smaller. The cause of these changes in the viscosity at a shear rate of 10^{-2} s^{-1} will be discussed in detail later from the viewpoint of the amount of CMC adsorbed on graphite following the dynamic viscoelasticity results.

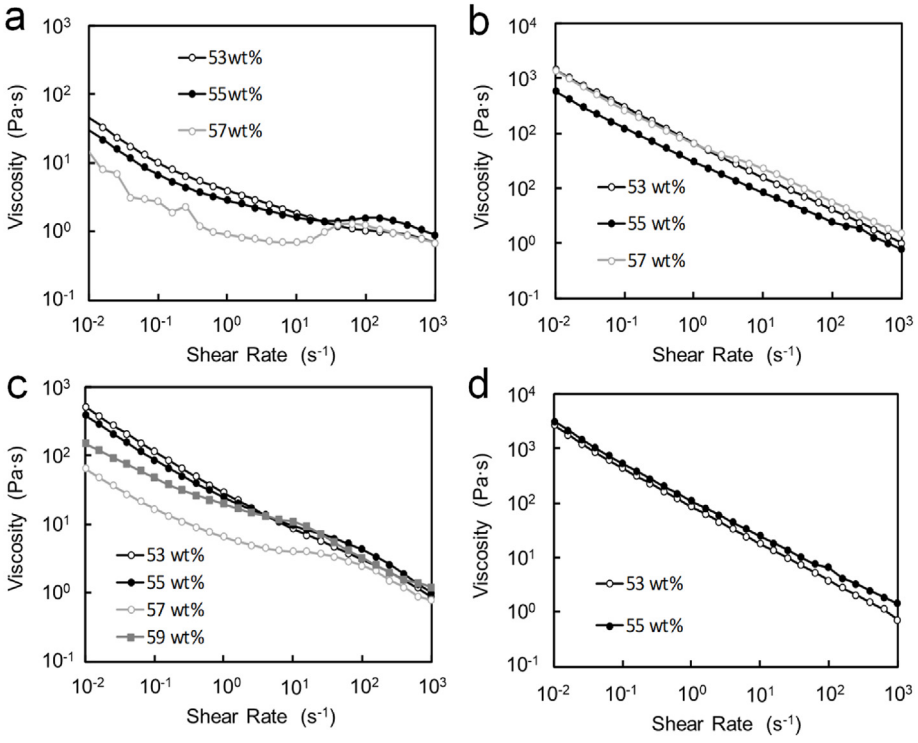

Fig. 3. Viscosities as functions of shear rate for model anode slurries with CMC concentrations of (a) 0.2, (b) 0.4, (c) 0.6 and (d) 0.8 wt% using CMC-C. The wt% values shown in the graphs indicate graphite concentrations.

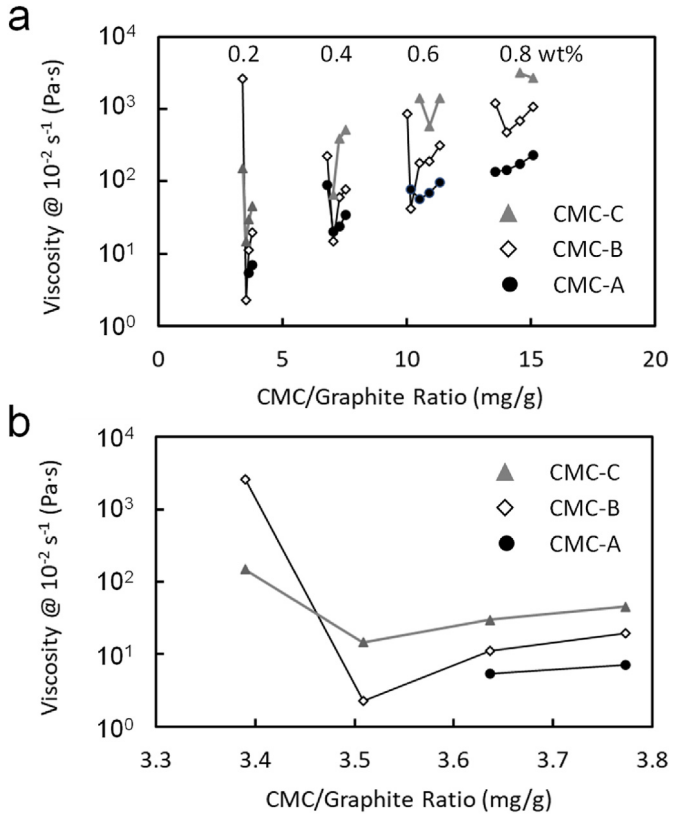

Fig. 4. (a) Relationship between viscosity at 10^{-2} s^{-1} and weight ratio of CMC to graphite for all CMC concentrations. The wt% values shown in the graph indicate CMC concentrations. (b) Enlarged graph of 0.2 wt% part.

To clarify the impact of the CMC molecular weight and concentration on shear thickening, the strain dependence of G′ and G″ was measured. Fig. 5 shows the shear rate dependence of the viscosity and the strain dependence of G′ and G″ for the slurries containing the three CMCs, for a graphite concentration of 57 wt% and a CMC concentration of 0.6 wt%. Fig. 5a clearly demonstrates that only the CMC-A sample exhibited shear thickening accompanied by an increase in viscosity. However, the elastic moduli data in Fig. 5b and c confirm that strain hardening appeared along with an increase in the elastic modulus. This effect was especially evident in the loss modulus, G″, in the high strain region for each slurry. Since the strain hardening seen in the present work occurred as a result of shear thickening [33], the change in the value of G″ was used as an index of the degree of shear thickening. Specifically, the ratio of the maximum value of G″, G''_{max}, to the minimum value of G″, G''_{min}, in the strain region between 10^1 and 10^3% was used as the index.

Here, to clarify the effects of CMC molecular weight, CMC concentration, and graphite concentration on shear thickening, the values of G''_{max}/G''_{min} were plotted against the CMC/graphite ratio, as shown in Fig. 6. Measurement data for the strain dependence of the elastic modulus, on which these plots are based, are provided in Fig. S2 of the Supplementary Data. The graphs in Fig. 6 present that the degree of shear thickening tends to increase as the CMC/graphite ratio is decreased. The graphs also indicate that slurries containing high molecular weight CMCs tend to have less degree of shear thickening. In addition, the graphs indicate that the higher the CMC concentration, the smaller the degree of shear thickening, since the higher the CMC concentration, the smaller the scale on the vertical axis. These results suggest that CMCs adsorbed on graphite particles has a great effect on shear thickening.

4. Discussion

First, we consider the decrease in viscosity as the graphite concentration was increased from 53 to 57 wt%, for which there are two

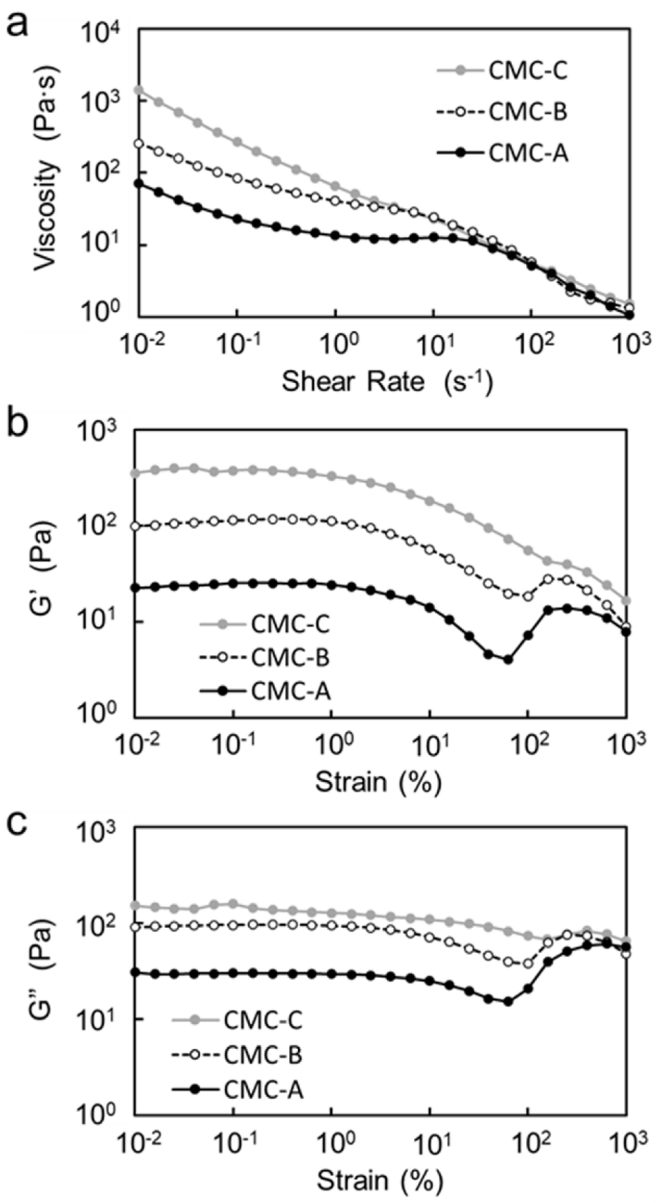

Fig. 5. (a) Viscosities as functions of shear rate and (b) storage modulus, and (c) loss modulus values as functions of strain for model anode slurries containing the three CMCs with a graphite concentration of 57 wt% and a CMC concentration of 0.6 wt%.

possible causes. One is the effect of CMC dispersed in the water on the viscosity. As the graphite concentration was increased, the amount of CMC that could be adsorbed on the graphite particles would have increased, such that the quantity of CMC dispersed in the water decreased. This effect, in turn, may have reduced the viscosity of the slurry. Another possible cause is the effect of CMC adsorption on the graphite. As the graphite concentration was increased, the mass of CMC adsorbed per graphite particle would have decreased so that the interactions of the adsorbed CMC were reduced and the viscosity was decreased. In order for this hypothesis to hold, most of the CMC molecules must be adsorbed on graphite particles in the slurry at any CMC concentration.

Fig. 7 shows the effects of shear rate on the viscosities of a model anode slurry having a graphite concentration of 55 wt% and an aqueous CMC dispersion. In the low shear rate range of 10^{-2} to 10^{0} s^{-1}, higher CMC concentrations increased the viscosity in both the slurries and the aqueous dispersions. These results indicate that the CMC itself was responsible for the rise in viscosity. However, focusing on the high shear

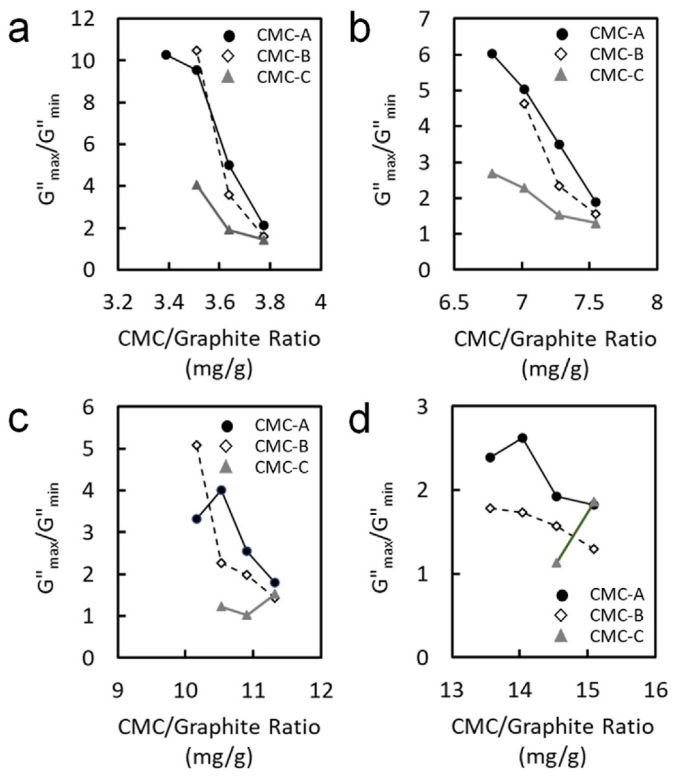

Fig. 6. G″max/G″min values as functions of weight ratio of CMC to graphite. CMC concentrations are 0.2 (a), 0.4 (b), 0.6 (c), and 0.8 wt% (d).

rate range around 10^3 s^{-1}, higher CMC concentrations in the aqueous dispersions increased the viscosity whereas the viscosities of the model slurries remained essentially constant. In the high shear rate region, the effects of the interactions between particles on the viscosity were minimized due to the high shear flow, and so the viscosity was primarily determined by the dispersion medium and the hydrodynamics resulting from the solids content [34]. Therefore, the observation that the viscosities of the model slurries in the high shear rate range were generally unchanged suggests that the dispersion medium viscosities remained almost the same regardless of the CMC concentration. That is, it appears that the majority of the CMC added to the model slurries was adsorbed on the graphite, at least up to a CMC concentration of 0.8 wt%. It has been reported that the microstructure in a graphite/CMC slurry having a graphite concentration of 50 wt% can be explained by the characteristics of CMC adsorbed on graphite up to a CMC concentration of about 1.3 wt % [29]. Thus, we conclude that the decreases in viscosity with increases in graphite concentration from 53 to 57 wt% in the present experiments did not result from decreases in dispersed CMC but rather from a lower amount of CMC adsorbed on each graphite particle. This decrease in adsorbed CMC per particle in turn reduced the electrostatic and steric interactions between graphite particles induced by the adsorbed CMC [27]. The rapid increase in viscosity at a graphite concentration of 59 wt % as shown in Figs. 1b, 2a and 2b is ascribed to particle agglomeration resulting from the weakened interactions between the graphite particles because of the further decrease in the amount of CMC adsorbed per particle. This agglomeration made it impossible to maintain a stable dispersion. As described above, by considering the change in the amount of adsorbed CMC, it is possible to explain both the decrease in viscosity in the low shear rate range due to the increase in particle concentration and the rapid increase in viscosity due to further increase in particle concentration at the same CMC concentration.

Next, the effects of CMC species, CMC concentration, and graphite concentration on shear thickening will be discussed focusing the amount of adsorbed CMC. When the CMC concentration was relatively low and the graphite concentration was relatively high, in conjunction with a low molecular weight CMC, the degree of shear thickening tended to be large. Shear thickening is essentially a manifestation of changes in the balance of forces, due to the formation of clusters and interconnection between clusters [35]. As one model to explain the shear thickening caused by such a change in the balance of forces, a friction model has recently been reported, in which increases in viscosity occur due to friction generated when particles undergoing shear collide with one another [36–39]. This model has been supported by many experimental trials [40–47]. Our results can also be qualitatively explained based on this model, assuming that the CMC adsorbed on the graphite particles acted as a buffer layer to suppress shear thickening. In the case that the CMC concentration was low or the graphite particle concentration was high, the amount of CMC adsorbed on each particle would have been reduced and so the buffering effects of the CMC would not have been as pronounced so that sheer thickening occurred. Conversely, a high CMC concentration and low graphite particle concentration generated a large quantity of CMC on each graphite particle, such that shear thickening was inhibited. Because the reduction of shear thickening was greater in slurries containing the CMC-C (which had a higher molecular weight), it appears that the ability of the adsorbed CMC to act as a buffer layer can be attributed to steric forces rather than electrostatic interactions, in agreement with a previous report [27].

The above discussions are summarized by the diagram in Fig. 8. In this mechanism, when the CMC concentration is low (lower part of Fig. 8) together with a low graphite concentration, the aggregation of graphite particles is suppressed by the adsorption of a sufficient amount of CMC. As the graphite concentration increases, the amount of adsorbed CMC per graphite particle decreases (Fig. 8, lower center). As a result, the interactions between particles are weakened, the viscosity in the low shear rate region is decreased and shear thickening appears in the high shear

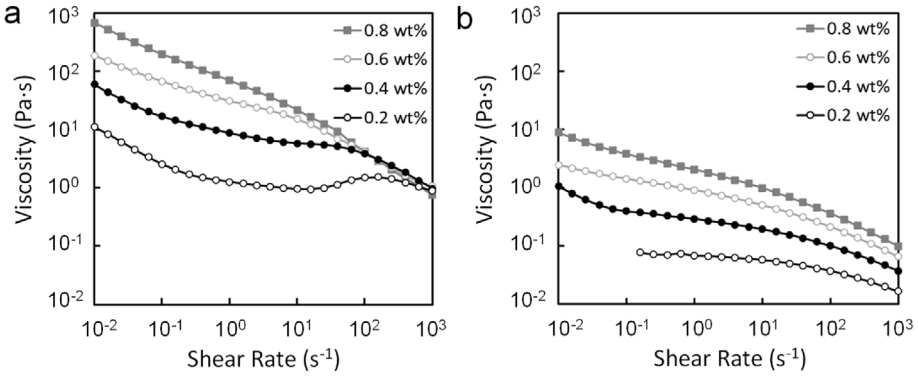

Fig. 7. Viscosities as functions of shear rate for (a) model anode slurries with a graphite concentration of 55 wt% and (b) CMC suspensions, using CMC-B. The values in the graphs indicate CMC concentrations.

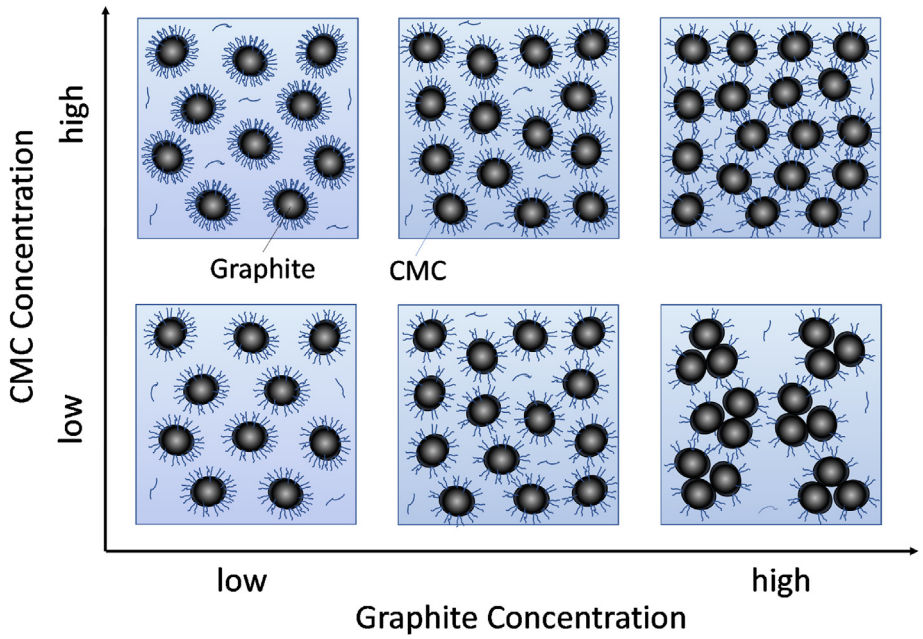

Fig. 8. A schematic diagram of graphite particles adsorbed by CMC in the model slurries.

rate region. Further increases in the graphite concentration provide additional decreases in the amount of adsorbed CMC on each particle, such that interactions between graphite particles are weakened and aggregation occurs (Fig. 8, lower right), resulting in an increase in viscosity and fluctuations in the data. At elevated CMC concentrations (upper part of Fig. 8), even if the graphite concentration is high and the amount of CMC adsorbed per graphite particle is reduced, sufficient CMC adsorption is maintained for dispersion. Consequently, the viscosity does not increase significantly and shear thickening within the high shear rate range is also suppressed. The CMC having the highest molecular weight (CMC-C) provided the strongest steric interactions and therefore had a greater effect on viscosity and shear thickening.

5. Conclusions

The effects of CMC adsorption on graphite particles on the rheological properties of model anode slurries were examined by monitoring the viscoelasticity of slurries having different graphite concentrations, CMC molecular weights and CMC concentrations. The experimental results show that, at a specific CMC concentration, raising the graphite concentration from 53 to 57 wt% decreases the viscosity in the low shear rate while increasing shear thickening in the high shear rate range. It is also evident that higher CMC molecular weights reduce the degree of shear thickening. These results suggest that the majority of the CMC is adsorbed on the graphite particles, at least up to a CMC concentration of 0.8 wt %. In the low shear rate range, this adsorbed CMC contributes to the development of viscosity through electrostatic and steric interactions while, in the high shear rate range, it acts as a buffer to suppress particle collisions and reduce shear thickening. The steric interactions resulting from the adsorbed CMC evidently determine the rheological properties of the slurry because shear thickening is suppressed to a greater extent by a CMC having a higher molecular weight.

Declaration of competing interest

The authors declare that they have no known competing financial interests or personal relationships that could have appeared to influence the work reported in this paper.

Acknowledgements

The author thanks TOYOTA Central Res. & Develop. Labs., Inc., Japan for funding the project and grateful to the Slurry Research Division for helpful discussions regarding the experimental results.

Appendix A. Supplementary data

Supplementary data to this article can be found online at https://doi.org/10.1016/j.jciso.2022.100048.

References

[1] E. Brown, H.M. Jaeger, Shear thickening in concentrated suspensions: phenomenology, mechanisms and relations to jamming, Rep. Prog. Phys. 77 (2014), 046602.
[2] A. Glasser, É. Cloutet, G. Hadziioannou, H. Kellay, Tuning the rheology of conducting polymer inks for various deposition processes, Chem. Mater. 31 (2019) 6936–6944.
[3] S. Latorrata, P.G. Stampino, E. Amici, R. Pelosato, C. Cristiani, G. Dotelli, Effect of rheology controller agent addition to Micro-Porous Layers on PEMFC performances, Solid State Ionics 216 (2012) 73–77.
[4] W. Bauer, D. Nötzel, Rheological properties and stability of NMP based cathode slurries for lithium ion batteries, Ceram. Int. 40 (2014) 4591–4598.
[5] K. Dimic-Misic, P.A.C. Gane, J. Paltakari, Micro- and nanofibrillated cellulose as a rheology modifier additive in CMC-containing pigment-coating formulations, Ind. Eng. Chem. Res. 52 (2013) 16066–16083.
[6] L. Jin, Y. Shangguan, T. Ye, H. Yang, Q. An, Q. Zheng, Shear induced self-thickening in chitosan-grafted polyacrylamide aqueous solution, Soft Matter 9 (2013) 1835–1843.
[7] M. Yu, X. Qiao, X. Dong, K. Sun, Shear thickening effect of the suspensions of silica nanoparticles in PEG with different particle size, concentration, and shear, Colloid Polym. Sci. 296 (2018) 1119–1126.
[8] E. Brown, N.A. Forman, C.S. Orellana, H. Zhang, B.W. Maynor, D.E. Betts, J.M. DeSimone, H.M. Jaeger, Generality of shear thickening in dense suspensions, Nat. Mater. 9 (2010) 220–224.
[9] S. Khandavalli, J.P. Rothstein, Large amplitude oscillatory shear rheology of three different shear-thickening particle dispersions, Rheol. Acta 54 (2015) 601–618.
[10] Y.S. Lee, N.J. Wagner, Dynamic properties of shear thickening colloidal suspensions, Rheol. Acta 42 (2003) 199–208.
[11] F. Toussaint, C. Roy, P.-H. Jézéquel, Reducing shear thickening of cement-based suspensions, Rheol. Acta 48 (2009) 883–895.
[12] J.A. Lewis, Colloidal processing of ceramics, J. Am. Ceram. Soc. 83 (2000) 2341–2359.
[13] A. Benchabane, K. Bekkour, Effects of anionic additives on the rheological behavior of aqueous calcium montmorillonite suspensions, Rheol. Acta 45 (2006) 425–434.

[14] W.N. Sharratt, R. O'Connell, S.E. Rogers, C.G. Lopez, J.T. Cabral, Conformation and phase behavior of sodium carboxymethyl cellulose in the presence of mono- and divalent salts, Macromolecules 53 (2020) 1451–1463.
[15] C.G. Lopez, W. Richtering, Influence of divalent counterions on the solution rheology and supramolecular aggregation of carboxymethyl cellulose, Cellulose 26 (2019) 1517–1534.
[16] C.G. Lopez, Entanglement properties of polyelectrolytes in salt-free and excess-salt solutions, ACS Macro Lett. 8 (2019) 979–983.
[17] C.G. Lopez, R.H. Colby, J.T. Cabral, Electrostatic and hydrophobic interactions in NaCMC aqueous solutions: effect of degree of substitution, Macromolecules 51 (2018) 3165–3175.
[18] C.G. Lopez, R.H. Colby, P. Graham, J.T. Cabral, Viscosity and scaling of semiflexible polyelectrolyte NaCMC in aqueous salt solutions, Macromolecules 50 (2017) 332–338.
[19] C.G. Lopez, S.E. Rogers, R.H. Colby, P. Graham, J.T. Cabral, Structure of sodium carboxymethyl cellulose aqueous solutions: a SANS and rheology study, J. Polym. Sci. B Polym. Phys. 53 (2015) 492–501.
[20] D. Truzzolillo, F. Bordi, C. Cametti, S. Sennato, Counterion condensation of differently flexible polyelectrolytes in aqueous solutions in the dilute and semidilute regime, Phys. Rev. E - Stat. Nonlinear Soft Matter Phys. 79 (2009), 011804.
[21] A. Benchabane, K. Bekkour, Rheological properties of carboxymethyl cellulose (CMC) solutions, Colloid Polym. Sci. 286 (2008) 1173–1180.
[22] X.H. Yang, W.L. Zhu, Viscosity properties of sodium carboxymethylcellulose solutions, Cellulose 14 (2007) 409–417.
[23] C. Clasen, W.-M. Kulicke, Determination of viscoelastic and rheo-optical material functions of water-soluble cellulose derivatives, Prog. Polym. Sci. 26 (2001) 1839–1919.
[24] W.-M. Kulicke, A.H. Kull, W. Kull, H. Thielking, Characterization of aqueous carboxymethylcellulose solutions in terms of their molecular structure and its influence on rheological behaviour, Polymer 37 (1996) 2723–2731.
[25] J. Drofenik, M. Gaberscek, R. Dominko, F.W. Poulsen, M. Mogensen, S. Pejovnik, J. Jamnik, Cellulose as a binding material in graphitic anodes for Li ion batteries: a performance and degradation study, Electrochim. Acta 48 (2003) 883–889.
[26] J.-H. Lee, S. Lee, U. Paik, Y.-M. Choi, Aqueous processing of natural graphite particulates for lithium-ion battery anodes and their electrochemical performance, J. Power Sources 147 (2005) 249–255.
[27] J.-H. Lee, U. Paik, V.A. Hackley, Y.-M. Choi, Effect of carboxymethyl cellulose on aqueous processing of natural graphite negative electrodes and their electrochemical performance for lithium batteries, J. Electrochem. Soc. 152 (2005) A1763–A1769.
[28] C.-C. Li, Y.-S. Lin, Interactions between organic additives and active powders in water-based lithium iron phosphate electrode slurries, J. Power Sources 220 (2012) 413–421.
[29] S. Lim, S. Kim, K.H. Ahn, S.J. Lee, The effect of binders on the rheological properties and the microstructure formation of lithium-ion battery anode slurries, J. Power Sources 299 (2015) 221–230.
[30] W.J. Chang, G.H. Lee, Y.J. Cheon, J.T. Kim, S.I. Lee, J. Kim, M. Kim, W.I. Park, Y.J. Lee, Direct observation of carboxymethyl cellulose and styrene butadiene rubber binder distribution in practical graphite anodes for Li-ion batteries, ACS Appl. Mater. Interfaces 11 (2019) 41330–41337.
[31] R. Gordon, R. Orias, N. Willenbacher, Effect of carboxymethyl cellulose on the flow behavior of lithium-ion battery anode slurries and the electrical as well as mechanical properties of corresponding dry layers, J. Mater. Sci. 55 (2020) 15867–15881.
[32] J. He, H. Zhong, J. Wang, L. Zhang, Investigation on xanthan gum as novel water soluble binder for LiFePO 4 cathode in lithium-ion batteries, J. Alloys Compd. 714 (2017) 409–418.
[33] M. Ishii, H. Nakamura, Applicability of modified cox-merz rule to concentrated suspensions, J. Non-Newtonian Fluid Mech. 282 (2020), 104322.
[34] J. Mewis, N.J. Wagner, Colloidal Suspension Rheology, Cambridge University Press, Cambridge, 2011.
[35] A. Zaccone, D. Gentili, H. Wu, M. Morbidelli, E. Del Gado, Shear-driven solidification of dilute colloidal suspensions, Phys. Rev. Lett. 106 (2011), 138301.
[36] R. Mari, R. Seto, J.F. Morris, M.M. Denn, Shear thickening, frictionless and frictional rheologies in non-Brownian suspensions, J. Rheol. 58 (2014) 1693–1724.
[37] R. Seto, R. Mari, J.F. Morris, M.M. Denn, Discontinuous shear thickening of frictional hard-sphere suspensions, Phys. Rev. Lett. 111 (2013), 218301.
[38] R. Mari, R. Seto, J.F. Morris, M.M. Denn, Nonmonotonic flow curves of shear thickening suspensions, Phys. Rev. E - Stat. Nonlinear Soft Matter Phys. 91 (2015), 052302.
[39] R. Mari, R. Seto, J.F. Morris, M.M. Denn, Discontinuous shear thickening in Brownian suspensions by dynamic simulation, Proc. Natl. Acad. Sci. U. S. A. 112 (2015) 15326–15330.
[40] B.M. Guy, M. Hermes, W.C. Poon, Towards a unified description of the rheology of hard-particle suspensions, Phys. Rev. Lett. 115 (2015), 088304.
[41] H. Nakamura, S. Makino, M. Ishii, Continuous shear thickening and discontinuous shear thickening of concentrated monodispersed silica slurry, Adv. Powder Technol. 31 (2020) 1659–1664.
[42] H. Nakamura, S. Makino, M. Ishii, Effects of electrostatic interaction on rheological behavior and microstructure of concentrated colloidal suspensions, Colloids Surf. A Physicochem. Eng. Asp. 623 (2021), 126576.
[43] A. Vazquez-Quesada, R.I. Tanner, M. Ellero, Shear thinning of noncolloidal suspensions, Phys. Rev. Lett. 117 (2016), 108001.
[44] C. Clavaud, A. Berut, B. Metzger, Y. Forterre, Revealing the frictional transition in shear-thickening suspensions, Proc. Natl. Acad. Sci. U. S. A. 114 (2017) 5147–5152.
[45] A.K. Townsend, H.J. Wilson, Frictional shear thickening in suspensions: the effect of rigid asperities, Phys. Fluids 29 (2017), 121607.
[46] G. Chatte, J. Comtet, A. Nigues, L. Bocquet, A. Siria, G. Ducouret, F. Lequeux, N. Lenoir, G. Ovarlez, A. Colin, Shear thinning in non-Brownian suspensions, Soft Matter 14 (2018) 879–893.
[47] C.P. Hsu, J. Mandal, S.N. Ramakrishna, N.D. Spencer, L. Isa, Exploring the roles of roughness, friction and adhesion in discontinuous shear thickening by means of thermo-responsive particles, Nat. Commun. 12 (2021) 1477.